PNNL-13696

Pacific Northwest
National Laboratory
Operated by Battelle for the
U.S. Department of Energy

Experimental Investigation of Continuous-Wave Laser Ionization of Kryption

B. D. Cannon
R. F. Shannon, Jr.

October 2001

Prepared for the U.S. Department of Energy
under Contract DE-AC06-76RL01830

DISCLAIMER

PACIFIC NORTHWEST NATIONAL LABORATORY
operated by
BATTELLE
for the
UNITED STATES DEPARTMENT OF ENERGY
under Contract DE-ACO6-76RLO183O

Printed in the United States of America

Available to DOE and DOE contractors from the
Office of Scientific and Technical Information,
P.O. Box 62, Oak Ridge, TN 37831-0062;
ph: (865) 576-8401
fax: (865) 576-5728
email: reports@adonis.osti.gov

Available to the public from the National Technical Information Service,
U.S. Department of Commerce, 5285 Port Royal Rd., Springfield, VA 22161
ph: (800) 553-6847
fax: (703) 605-6900
email: orders@ntis.fedworld.gov
online ordering: http://www.ntis.gov/ordering.htm


This document was printed on recycled paper.
(8/00)

PNNL-13696

Experimental Investigation of Continuous-Wave Laser Ionization of Krypton

B. D. Cannon
R. F. Shannon, Jr.

September 2001

Prepared for
the U.S. Department of Energy
under Contract DE-AC06-76RLO 1830

Pacific Northwest National Laboratory
Richland, Washington 99352

Summary

This report describes experimental investigations of a method that uses continuous-wave lasers to ionize selected isotopes of krypton with high isotopic selectivity. The experiments showed that the ionization rate is at least a factor of 100 lower than was calculated with our model, which was described in a previous report (Cannon 1999). This discrepancy may be due to a much smaller excitation cross-section than expected based on previous work and/or the aberrations in the ultraviolet beam used for the first step in the excitation. Additional problems with damage to mirrors, alignment instabilities, and manufacturers halting production of key products make this approach not worth further development at this time.

Acknowledgment

This research was sponsored by the U.S. Department of Energy, Office of Nonproliferation and National Security, Office of Research and Development (NN-20). Pacific Northwest National Laboratory is operated by Battelle for the U.S. Department of Energy.

Contents

Figures

1.0 Introduction

This report describes experiments to demonstrate efficient and isotopically selective ionization of krypton with continuous-wave (CW) lasers and to verify our previously reported modeling of this approach (Cannon 1999). The results of these model calculations predicted that combining this ionization scheme with mass spectrometric measurement of the resulting ions could be the basis for ultra-sensitive methods to measure the minor krypton isotopes. However, in two different experiments, no evidence for laser ionization of krypton was observed, while our model predicted signal-to-noise ratios of greater than 100. Subsequent measurements indicate that aberrations in the ultraviolet (UV) beam used for the first excitation step may be largely responsible for the lack of signal. Additional problems with several aspects of the experiment and planned upgrades were also discovered, indicating that this approach does not merit further development at this time

This report will first describe the laser ionization scheme, the experimental setups, and the performance of the two key pieces of apparatus. Then it will present the results of experiments to observe laser ionization of krypton and, finally, detailed discussions of the problems found in this approach.

2.0 Excitation Scheme

Figure 2.1 shows the two excitation schemes used in our experiments, which are simplified versions of the scheme considered in our model (Cannon 1999). Both schemes start with CW single-frequency light with a wavelength of 214.7681 nm exciting krypton atoms in the ground state, $1p_0$, to an excited state, $2p_6$, by a two-photon transition. Because this first transition is a two-photon transition, the excitation rate is proportional to the square of the irradiance (power per unit area). A two-photon excitation offers the potential for Doppler-free excitation, which can provide increased isotopic selectivity and higher excitation rates for a given irradiance. To increase the irradiance and thus the excitation rate and to provide the equal intensity counter-propagating beams needed for efficient Doppler-free two-photon excitation, we used a buildup cavity. Approximately 70% of the atoms excited to the $2p_6$ state radiate to the metastable $1s_5$, state while the remainder return to the ground state by way of one of two short lived intermediate states (Chang et al. 1980). The radiative lifetime of the $2p_6$ state is 26.2 ns (Whitehead 1992), while that of the $1s_5$ state is calculated to be 85 seconds (Small-Warren and Chiu 1975), which means that in a vacuum system the time available to ionize the metastable state is determined by the

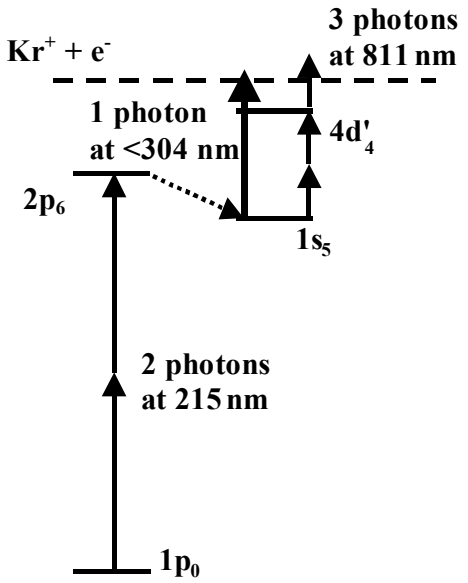

Figure 2.1. Schematic Diagram of Excitation Schemes. Two-photon excitation near 215 nm selectively excites krypton atoms of a desired isotope from the $1p_0$ ground state to the $2p_6$ state from which they decay by spontaneous emission to the metastable $1s_5$ state. A second laser beam then photoionizes the atoms in the $1s_5$ state. For some experiments, this second laser beam comprised the deep UV lines from an argon ion laser, while for the rest of the experiments it was a tunable laser near 811 nm. This 811 nm beam selectively excites the desired krypton isotope from the $1s_5$ state to the $4d_4'$ state and then ionizes it. The energy level splittings of the six stable krypton isotopes in the $1p_0$ - $2p_6$ and $1s_5$ - $4d_4'$ transitions are resolvable with the lasers used but are not shown. For both two-photon transitions, the laser wavelengths were scanned over the wavelengths of the major isotopes.

transit time across the ionizing laser beam, which is approximately a factor of 100 times longer than the radiative lifetime of the $2p_6$. The atoms in the $1s_5$ state are subsequently ionized either directly with the deep ultraviolet lines from an argon ion laser (302.4 nm and 275.4 nm) or via the $4d_4'$ state by light at 811 nm. One of us has previously studied this later path for ionizing the metastable $1s_5$ state of krypton (Cannon and Janik 1988; Cannon et al. 1993), and it is calculated to be much more efficient for ionizing the krypton metastable. This larger ionization efficiency results from the extremely large cross-section for the two-photon transition to the $4d_4'$ state, the large photo-ionization cross-section of the $4d_4'$ state, and the ability to overlap a focused 811 nm laser beam with the UV beam used for the first transition.

3.0 Experimental Setup

Figure 3.1 shows a schematic diagram of the experimental setup for looking for CW laser ionization of krypton. A commercial, single-frequency, CW, dye laser (Coherent Model 699-21) produces approximately 250 mW of light with a wavelength near 430 nm that is frequency-doubled in an external cavity frequency-doubler for CW lasers (Spectra Physics WaveTrain™). The wavelengths of the single-frequency lasers are measured with a wavelength meter (Burleigh Model WA-1500) to 0.2 parts per million. The extremely elliptical beam exiting the cavity of this frequency doubler is approximately circularized with a pair of cylindrical lenses within the WaveTrain. A plano-concave fused-silica lens with a focal length of –1 m and a two-element air-spaced fused-silica lens with a 200 mm focal length (OptoSigma Part # 027-2260) were used to match the laser spatial mode to the mode of the UV enhancement cavity, which is in the vacuum system. The 215 nm beam transmitted by the enhancement cavity hits a photodiode that was part of the electronics to lock this cavity to the frequency of the 215-nm beam. For experiments using the deep UV lines from an argon ion laser for ionization, that beam was approximately 3 mm in diameter, had 0.45 W of power, and perpendicularly intersected the 215 nm beam in the enhancement cavity. For these experiments, the vacuum chamber was filled with krypton at a pressure of approximately 1 x 10^{-4} Torr by using a leak valve and partially closing the gate valve to the pump. For experiments using 811-nm light for ionization, 0.3 W from a single-frequency titanium-sapphire laser (Coherent Model 899-21) was made to overlap and counter-propagate with the 215-nm beam and was focused into the middle of the enhancement cavity, whose mirrors have low reflectivity at 811 nm, to a beam diameter of approximately 0.1 mm. For these experiments, the krypton entered the enhancement cavity in an effusive atomic beam from a micro-capillary array, which had a calculated divergence of 80 mrad and an estimated number density of 10^{14} cm^{-3} at the 215-nm beam.

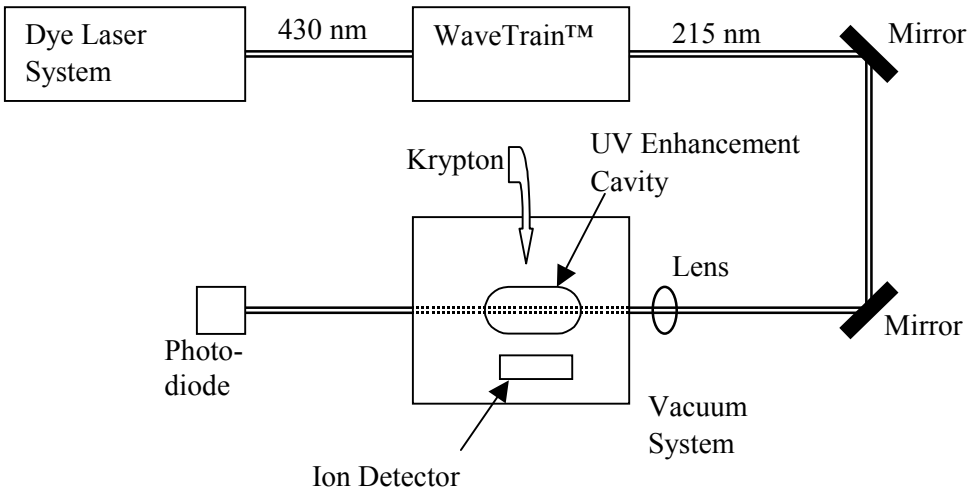

Figure 3.1. Schematic Diagram of Experiment to Observe CW Laser Ionization of Krypton. Frequency doubling light from a single-frequency dye laser system in a WaveTrain external cavity doubler generates UV with a wavelength near 215 nm for the two-photon excitation of krypton.

The dye-laser/WaveTrain system can produce up to 6 mW of frequency-doubled light at 214.768 nm; however, for the experiments on ionization of krypton, only 3.7 mW was incident on the UV enhancement cavity in the vacuum system. This reduced power was due to alignment instabilities in the dye laser and WaveTrain and losses in the optics between the WaveTrain and the UV enhancement cavity. Even minor adjustments in the optical alignment of the dye laser to optimize power change the pointing of the dye laser beam enough to require adjusting the alignment of the WaveTrain, which then requires adjusting the alignment into the UV enhancement cavity. A modern replacement for the 699-21, which was first produced in the late 1970s, that has a more stable optical alignment would be required if one is to spend more time each day making measurements than is spent aligning optics.

The enhancement cavity in the vacuum system accepted the incident power in the 215-nm beam from the WaveTrain and built it up by factors of up to 60 within the cavity. This enhancement cavity consisted of a pair of high-reflectivity concave mirrors for 214.7 nm with radii of curvature of 15 mm that were made by Alpine Research Optics. The 6.35 mm in diameter by 3 mm thick substrates for these mirrors are made of excimer grade fused silica and the backsides are flat and have an anti-reflection coating for 214.7 nm. These mirrors were mounted in mounts (Thor Labs Model KC-1) that had been customized by the manufacture to be vacuum compatible. The mounts were attached to 4 stainless steel (SS) rods (6.00 mm diameter) that extended 125 mm from a 25 mm thick SS disk that was welded to a 100 mm diameter SS tube whose other end was fastened to a 150 mm diameter Conflat™ flange. Sliding these mounts along the rods makes gross adjustments of the mirror spacing and turning the 1/4-80 alignment screws on the mounts makes fine adjustments. One of the mounts also had piezoelectric stacks that could be controlled by voltages applied to electrical feedthroughs in the Conflat flange on which this enhancement cavity was mounted. This piezo system (Thor Labs Model PZ631) was used to scan the cavity mirror separation for alignment and measurement of cavity finesse as well as to dither the mirror and make correction to the cavity spacing for the electronic locking of the cavity mirror spacing to the laser frequency. For all the laser ionization experiments, we used the enhancement cavity in the confocal geometry where the mirror separation equals the radii of curvature. We did try to align this enhancement cavity in the near-spherical geometry assumed in the modeling report (Cannon 1999), but the alignment tolerances are much more stringent in this case. After investing about two weeks trying to master this alignment, we decided that expected factors of 2 to 5 increase in excitation rate was not worthwhile for these initial experiments on laser ionization of krypton.

We used a “home-built” ion optic assembly and a quadrupole mass spectrometer (Extra Nuclear) with a channeltron detector for ion detection in our initial experiments. This ion optic assembly started with biasing the mirror mounts’ metal plates that held the mirrors to establish the initial ion potential energy. A kit from the manufacturer allowed these plates to be electrically isolated from the rest of the cavity assembly. An extractor, horizontal and vertical steering plates, and an einzel lens completed this ion optics assembly. This combined setup had a low background count rate of approximately 1 count per minute. However, when we were unable to see any krypton ion signals that were due to laser ionization with this setup, we became concerned that our ion optic system was not coupling the krypton ions into the quadrupole. To eliminate this possible problem, we changed to a using a bare channeltron with baffles to prevent 215-nm light scattered from the mirrors of the enhancement cavity from directly reaching the channeltron. This setup was very efficient in collecting ions, including those from the Bayard-Alpert pressure gauge when it was on, but had a background count rate of typically 300 counts per second.

The spatial profile of the 215 nm beam from the WaveTrain was measured using a UV-visible converter (Coherent Model BIP-12F) and a laser beam analyzer (Spiricon Model LBA-100A equipped with a Pulnix TM-7CN camera). A beam splitter (Coherent Model UV-B Cube) directed approximately 5% of the 215-nm beam onto the fluorescent screen of the converter. A software package (Spiricon LBA-300PC v2.54 demo) fit a Gaussian function to cuts through the data along the major and minor axes of the elliptical beams. We calibrated the distance scale of this beam analyzer setup by placing on the fluorescent screen a paper disk with a 6.3-mm-diameter hole in the center and illuminating with a 15-cm-long "black light." The ratio of the hole's diameter to that measured with the software was used to correct the beam sizes reported by the software.

4.0 Apparatus Performance

4.1 WaveTrain™

The frequency-doubled output power is proportional to the square of the input power for available dye laser powers when thermal effects and saturation are not significant. Thus the ratio of the doubled output power to the square of the input power is independent of the input power. We call this ratio the doubling efficiency coefficient. Figure 4.1 plots measurements of this coefficient for the WaveTrain versus dye laser wavelength collected on four days. For example, with a doubling efficiency coefficient of 6%/W and 0.25 W of dye laser power, the doubling efficiency is 1.5% and the doubled output power is 3.75 mW. Unfortunately, the wavelength of highest efficiency for the doubling crystal in our WaveTrain is approximately 2 nm longer than the wavelength we need. Another doubling crystal cut at a slightly different angle relative to the optical axis of the crystal could have its efficiency peaked at our wavelength of interest. However, specifying the wavelength of maximum doubling efficiency to less than 1 nm is not an option at this time. Most of the variability in these data at a specific wavelength comes from differences in the optical alignment. Each wavelength change requires a change in the tilt of the doubling crystal in WaveTrain to obtain maximum efficiency, which then requires adjustment of the mirrors in the

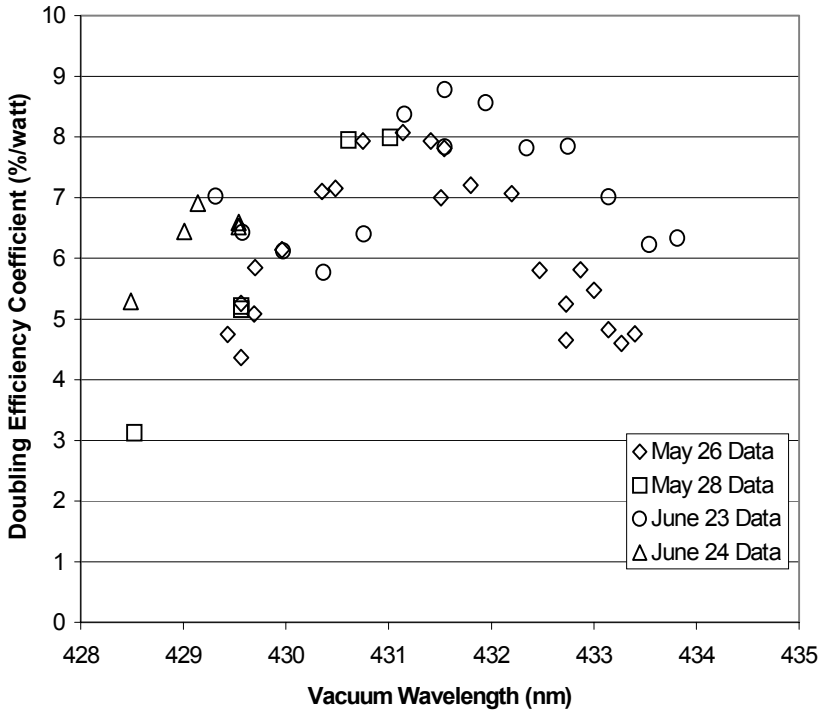

Figure 4.1. Doubling Efficiency Coefficient of WaveTrain Versus Vacuum Wavelength of Dye Laser. Data on the doubling efficiency for the WaveTrain used in this work measured as a function of dye laser wavelength on four separate days. The variations in the data result largely from variations in the optical alignment, which had to be readjusted for each change in wavelength.

WaveTrain's cavity and the position of the dye beam on the entrance mirror of this cavity. Because all of these adjustments interact, the optical alignment can be slow and tedious unless all the wavelengths of interest are within 0.01 nm.

We discovered two significant issues with the optical alignment of the WaveTrain that were not even mentioned in the manual. They both are related to small variations in the alignment of dye laser beam into the WaveTrain's cavity. The frequency-doubled beam exiting the cavity is highly elliptical with the ratio of the major axis to the minor axis of 15 60 cm from the doubling crystal. When properly aligned, the major axis is horizontal, but with minor errors in the input beam, alignment the major axis will rotate as much as 10° from horizontal without a major loss in achievable doubled power. This does, however, cause significant problems in using the cylindrical telescope to circularize the beam, which is necessary for efficient coupling into the UV enhancement cavity in the vacuum system. This same slight misalignment of the input also creates an offset in the electrical signal used for locking the WaveTrain's cavity to the laser frequency. This offset leads to a choice between maximum power with large power instabilities or low power with much better stability. The alignment method we finally developed required systematically varying the input beam alignment, adjusting the cavity mirrors and doubling crystal to get stable doubling, checking the tilt of the output beam and the offset of the locking signal, and then repeating the cycle to minimize both the tilt and offset. After the tilt and offset were minimized, the iterative process of adjusting the cavity mirrors, doubling crystal, and beam shifter for maximum power would begin. The first part of this process was needed only after a major dye laser alignment or something else caused a significant change in the pointing of the dye laser beam. The iterative adjustment for power was needed at the start of every day of experiments and often once or twice more during the day.

To efficiently couple the 215-nm light into the enhancement cavity and obtain the maximum irradiance in the cavity, the wave front of the beam incident on the input mirror of the cavity must closely match the wave front of the lowest order transverse electric mode (TEM_{00}) mode of the cavity. To attain this wave front matching, we measured the beam profile of the 215-nm beam as a function of distance and fit elliptical Gaussian profiles to these data. Figure 4.2 shows major and minor diameters found by these fits as functions of distance from the doubling crystal in the WaveTrain's cavity. These diameter data were fit by the equations

$$w(z) = w_0\sqrt{1+\left(\frac{z-z_w}{z_0}\right)^2}$$

$$z_0 = \frac{\pi {w_0}^2}{4M^2\lambda}$$

for the diameter of non-ideal Gaussian beam as a function of distance (Siegman 1986), where $w(z)$ is the beam diameter to $1/e^2$ as a function of position along the optical axis, z, w_0 is the beam diameter at the beam waist, z_w is the position of the waist along the optical axis, z_0 is the effective Rayleigh range, M^2 is the "times diffraction limited" parameter, and λ is the wavelength. The equation for z_0 has a factor of 4 in the denominator that is not in the more commonly written expression because these equations are in terms of diameter rather than radii. These data are well fit by an elliptical near-diffraction, limited Gaussian beam with the horizontal plane having the waist at the doubling crystal, a diameter to $1/e^2$ of 41 microns,

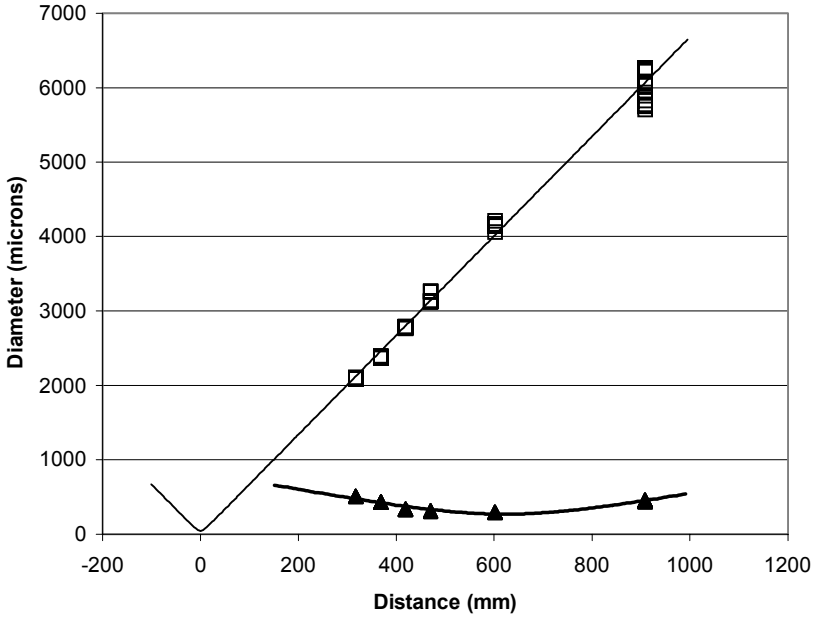

Figure 4.2. Diameters of the 215-nm Beam from the WaveTrain's Cavity. The diameters to 1/e2 along the major (hollow squares) and minor axes (solid triangles) of the elliptical beam from the WaveTrain's cavity are plotted as a function of distance from the doubling crystal. The lines are the expression for the size of a diffraction limited Gaussian beam fit to these data by varying the size and position of the beam waist.

and M^2=1; and, in the vertical plane, having the waist 620 mm from the doubling crystal, a diameter to $1/e^2$ of 268 microns, and M^2=1.25. The solid lines in Figure 4.2 are those given by the equations using the parameters (z_w, z_0, and M^2) found by least squares fitting to the data. The M^2 value in the horizontal plane could not be determined from the data because no data could be taken close to that waist; thus the beam was assumed to be diffraction limited in the horizontal plane. The differences in position and diameters of the waists in the vertical and horizontal planes need to be corrected for efficient coupling to the cylindrical mode of the enhancement cavity. We used parameters obtained from this fitting to guide our selection and initial placement of the optics to match the 215-nm beam mode to that of the cavity**.**

A telescope consisting of a pair of cylindrical lenses is part of the WaveTrain and was used to make the beam circular. Figure 4.3 shows beam diameters in the horizontal and vertical planes as a function of distance after the cylindrical telescope. These data show a nearly circular beam with the waists in the vertical and horizontal planes that are close together. The fits shown by the solid lines give M^2 values of 1.68 in both planes, waist diameters of 26 and 29 microns, and a 7.5 mm distance between them. These M^2 values are a little surprising because M^2 is preserved by a perfect optical system, and ray tracing of the elliptical beam through the cylindrical telescope with a commercial optical design program (Sinclair Optics' OSLO LT Version 5.2) shows very small aberrations. However, the data in Figure 4.3 were measured with a different alignment of the WaveTrain than was used for the data in Figure 4.2, so the difference in M^2 values may reflect changes in beam quality with WaveTrain alignment.

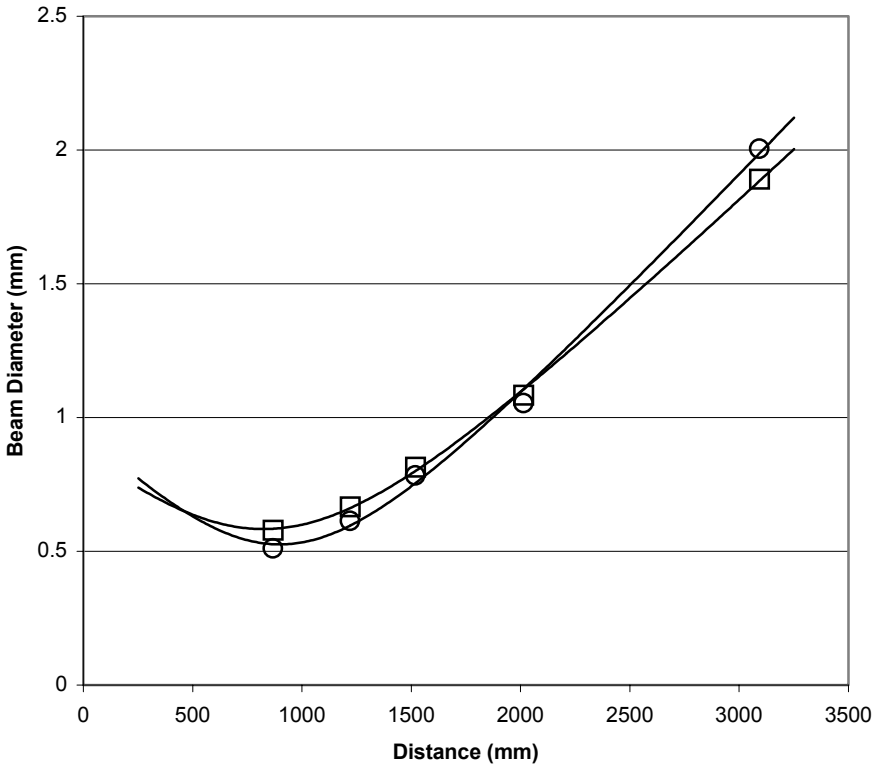

Figure 4.3. Size of Circularized 215-nm Beam Versus Distance. The beam diameters in the horizontal and vertical planes as a function of distance are well fit by the expression for Gaussian beams with M^2 of 1.68. The solid lines are the fit to the data.

Figure 4.4 shows measurements of a circularized 215-nm beam as it was focused for coupling into the enhancement cavity along with the fitted equations. In the least squares fitting, the M^2 parameters had to be constrained to be greater than or equal to 1 to prevent the non-physical result of M^2 much less than 1. This is probably a result of the small number of data points (only one more than the number of parameters) and the noise in the data. However, it could possibly indicate a more serious problem with some systematic error in our method. The fits give waists that are separated by 16 mm and have diameters of 64 microns and 48 microns for the minor and major axes respectively, and M^2 values of 1 for both axes. The data for Figure 4.4 was taken with a completely different alignment than the data for either Figure 4.2 or 4.3. The difference between the M^2 values for the data in Figures 4.3 and 4.4 is another indication that the 215-nm beam quality varies with the alignment of the WaveTrain.

4.2 UV Enhancement Cavity

Figure 4.4 also shows with a solid line the predicted mode size of the UV enhancement cavity in the confocal alignment that was used for almost all of our work. With the choice of the waist of the cavity mode centered between the waists of the focused 215-nm beam, there is a good match between the cavity

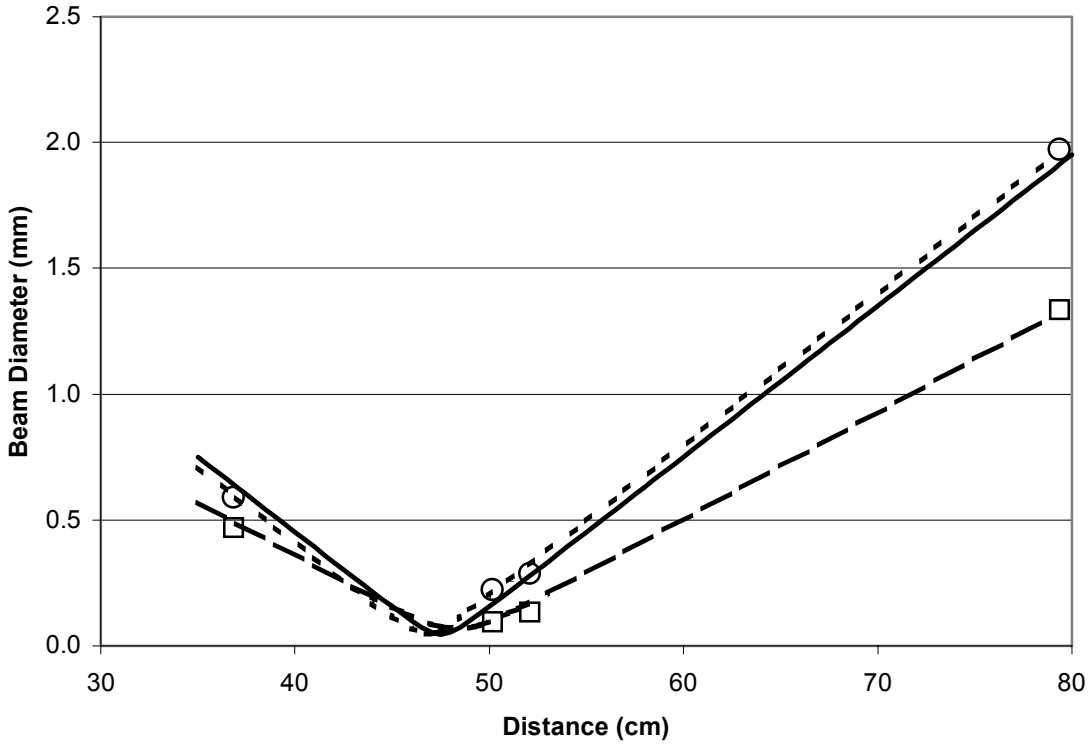

Figure 4.4. Beam Size of the 215-nm Beam Focused to Match the UV Enhancement Cavity. The plot shows the measured diameters along the major (hollow circles) and minor (hollow squares) axes of the elliptical beam that is focused down to match the mode of the UV enhancement cavity. Broken lines show the fits to these data, and the solid line shows the size of the mode of the UV enhancement cavity for the confocal alignment. The position of the waist of the enhancement cavity mode was chosen to be midway between the positions of the waists of the focused beam.

mode and the beam size. This is consistent with sharp and intense transmission peaks we observed when the system was properly aligned. In the case of no absorption or scatter by the cavity mirrors, the enhancement in a buildup cavity is given by the cavity finesse divided by π where the finesse is the ratio of the distance between successive longitudinal modes and the full width at half maximum of a transmission peak. A finesse of 130 is routinely achievable with our system in air, and values possibly as high as 200 have been observed. This indicates the possibility of enhancements of 40 to 60. The best method of measuring the true enhancement is to measure the transmission of only the output mirror and then the transmitted power when the cavity is locked to the incident beam. Using this method, our best estimates of the enhancement in the vacuum system are only about 7 to 8.

Several causes have been identified for the reduction from the potential to the observed enhancement, including misalignment and damage to mirrors while pumping down the vacuum system, vibrations of the cavity, and absorption and scatter by the mirrors. When the vacuum system containing the UV enhancement cavity is pumped down, the cavity becomes misaligned. A little of this misalignment is because the change in the refractive index going from air to vacuum requires a change in length to maintain the confocal alignment. The much larger effect is movement of the mirrors by airflow, out-gassing from around

the threads of the adjustment screws, and possibly deflection of the vacuum chamber itself due to the changed pressure differential. The piezoelectric adjustments that are on one mirror mount of the cavity are not enough to correct for these movements. The combination of intentional misalignment before pump-down and adjustment of the beam pointing can partially correct for this problem. However, adjusting the beam pointing requires that the 215-nm beam be incident on the cavity while pumping down. This results in damage to the cavity mirrors, apparently because the UV photolyzes something in the vacuum system that deposits on the mirrors, absorbs the UV, and thus reduces the enhancement. The material being "burned" onto the mirrors may be a component of the oil from the mechanical pump because once the turbo pump is running there seems to be no further damage to the mirrors.

Vibrations that come largely from the vacuum pumps create other problems that reduce the enhancement. To build up high circulating powers in an enhancement cavity, the separation between the mirrors must be an integral number times $\lambda/2$ to within a small fraction that is approximately 1 divided by 5 times the finesse. For example, with λ equal to 215 nm and a finesse of 100, the mirror separation needs to be held constant to 0.4 nm to have the transmission be between 86 and 100% of the maximum. The higher the finesse and hence the maximum possible enhancement, the more sensitive the cavity is to vibrations. To hold the cavity spacing to match the UV wavelength for the hour or more needed to search for a krypton ionization signal, we use a feedback circuit to lock the mirror separation to the UV wavelength. This is accomplished by applying a small dither to the piezoelectrics on the one mirror mount and using a locking amplifier to detect the change in transmission at the modulation frequency. Because of the slow response time of the mirror mount with the piezoelectrics, this feedback circuit can only correct for slow changes in cavity length. The lock becomes unstable if the finesse is too high.

5.0 Results and Discussion

5.1 Search for Krypton Ionization

Our initial experiments looking for a signal from laser ionization of krypton used deep UV from an argon ion laser for ionizing the krypton excited in the enhancement cavity and our "home-built" ion optics and the quadrupole mass spectrometer to detect the ions. Using the electron impact ionization apparatus that was part of the mass spectrometer, we confirmed that the quadrupole worked and was tuned to the krypton masses and that the ion detector and the counting electronics all worked. Many of these measurements were made with the DC voltage to the poles of the quadrupole turned off to pass a wide range of masses including the krypton masses. While this setup had a low background, less than one count per minute, we did not see any indication of a krypton ionization signal. We scanned the dye laser to cover the reported excitation energy (Cannon 1999; Trickl et al. 1989) for the most abundant krypton isotope, ^{84}Kr, of 93123.3295±0.0.0060 $cm^{-1}$and more than 0.1 cm^{-1} on either side of this value. This energy range covers not only many times the estimated uncertainty of the energy but also the previous reported energy for this transition. We made measurements both with a static pressure of krypton of almost 1 x 10^{-4} Torr and with our capillary array atomic beam. At that time we concluded that we must not have had the ion optics adjusted correctly, so we changed to our other ion detection setup.

Our second set of experiments looking for a krypton ionization signal used a bare channeltron, whose entrance was biased at about –1500 V, as the ion detector. Signals from the Bayard-Alpert ion gauge and scattered 215-nm light confirmed that the channeltron and counting electronics were working correctly. We looked for a krypton ionization signal using a static krypton pressure of almost 1 x 10^{-4} Torr and with deep UV from an argon ion laser for ionizing the krypton excited in the enhancement cavity. In these experiments, as well as in the first set, we scanned the 215-nm light more than 0.1 cm^{-1} on either side of the expected energy. Our model (Cannon 1999) predicts that, with our krypton atomic beam from the capillary array and using the 811 nm ionization path shown in Figure 2.1, the ion current should be 100 to 1000 times larger than it was in our previous experiments and about 10,000 times larger than our observed noise. So we tried this experiment with 811-nm light focused to overlap the 215-nm light in the enhancement cavity and still did not see any signal above the approximately 300 count per second level that represents three times the standard deviation of the background count rate.

5.2 Discussion

Great care is required to come to firm conclusions based on the failure to see a signal, such as in our experiments looking for CW laser ionization of krypton. Even if all the physics in our model (Cannon 1999) of these excitation and ionization processes is correct, there are many things that need to be working correctly, or at least well enough for us to see a krypton ionization signal. We know that the mass spectrometer and the detection electronics in the first set of experiments worked because we could detect krypton ions generated by the electron impact ionizer of the mass spectrometer. There is some uncertainty about whether our "home-built" ion optics were aligned to couple any krypton ions from the UV enhancement cavity into the mass spectrometer, even though we used the commercial ion optics simulation program SIMION to design and model them. With the second set of experiments, which used a bare channeltron for the ion detector, we are certain that we would have collected most of the ions

formed in the UV enhancement cavity. This was demonstrated by the channeltron's detecting ions escaping from the Bayard-Alpert ion gauge that had to travel through two right-angle elbows and then about 30 cm to reach this channeltron. Thus we are confident that the problem was that no krypton ions were being made, rather than that we were not detecting them.

The possible reasons for not ionizing krypton can be divided into two classes, problems either ionizing the atoms in the metastable state or exciting krypton ions to produce the $1s_5$ metastable state. Both of the processes we used for laser ionization of the krypton metastables have been studied previously using CW lasers. Hotop and coworkers (Kau et al. 1998) studied the ionization using deep UV from an argon ion laser, and Cannon and Janik (1988) studied the 811-nm ionization path. The long lifetime of the metastable state means there are no precision alignment requirements for either of these methods. For the 811-nm ionization method there is a precise requirement on the wavelength, but we performed computer-controlled grid searches of the wavelengths of both the 215- and 811-nm beams that covered regions that were much larger than the estimated uncertainties in both wavelengths. And so there is no obvious suspect in the ionization of the metastables. The production of the $1s_5$ metastables by two-photon excitation at 215 nm followed by spontaneous emission was studied with high-resolution laser with nanosecond long pulses (Wacker and Cannon 1991), and the two-photon cross-section used in our model was calculated by scaling those results. The laser bandwidth at 215 nm in those studies was a factor of approximately 300 larger than it was in this work, and the peak irradiances were approximately 20,000 times larger. In addition, in those pulsed measurements there was amplified spontaneous emission from the $2p_6$ that directly populated at least one lower state. Thus the two-photon cross-section seems the most uncertain piece of physics in our model.

Another source of uncertainty in the 215-nm excitation is the area of the beam in the UV enhancement cavity. We have no direct evidence that the size of the beam in the enhancement cavity matches that of the lowest order transverse electric mode (TEM_{00}) of the cavity. While for most cavities this would not be a question, it is for a confocal cavity because all the even transverse modes in a confocal cavity have the same set of mode frequencies as the TEM_{00} mode. This means that a confocal cavity can build up power in a much larger area than in a non-confocal cavity because it can simultaneously couple light from the incident beam into multiple transverse modes. The data shown in Figure 4.4 contradict this pessimistic possibility, but not as strongly as we would wish. There are only a few data points, and even the smallest diameter is twice the diameter of the waist found by the fit. This uncertainty is enhanced by the need to constrain the fit of these data to avoid obtaining the non-physical result of the beam being approximately 10 times better than diffraction limited.

The experiments with the largest predicted signal used the 811-nm ionization path and an atomic beam of krypton. This atomic beam was not directly characterized and thus might have had different characteristics than expected. We can estimate the flow of krypton through the capillary array nozzle from the pressure rise in the chamber when the krypton beam was turned on, the pumping speed of the turbo pump, and the conductance of the partially closed gate valve. However, it is possible that a mach disk formed between the nozzle exit and the 215-nm beam in the UV enhancement cavity because of the loss of conductance in the vicinity of the UV enhancement cavity from the mirror mounts obstructing the escape of the krypton. Such a mach disk would greatly attenuate the krypton beam and thus reduce the signal, but even from the static pressure in the vacuum chamber our model predicts a signal 20 times the observed noise level.

In addition to identifying possible problems based on our failure to observe a krypton ion signal, we can also draw some conclusions based on things we did observe. The amount of 215-nm power that we could reliably produce was about 4 mW, which is a factor of 25 less than the most optimistic level used in our model that predicted a useful ionization rate for krypton. To gain this factor of 25 increase in 215-nm power would require a tunable single-frequency 430-nm input of at least 1.25 W, which is well beyond any commercially available laser at the necessary wavelength. The original plan assumed we would achieve higher doubling efficiency to produce the 215-nm light than we achieved and that we would develop the necessary 430-nm source based on frequency-doubling the output of high-power diode laser amplifiers. Our experience with the WaveTrain makes the approach of generating more than 1.25 W of 430-nm light by frequency doubling look very difficult. In addition, the company that made high-power diode laser amplifiers has completely dropped that product line, which further complicates our original approach.

Our observed enhancements with the UV enhancement cavity were also significantly less than expected. While the observed finesse and transmission in air led us to expect enhancements of about 50, the observed enhancement in the vacuum system was only 7 to 8. Some of this difference could be reduced by a complete redesign of the mounting and alignment system of the cavity and major changes to the vacuum system to reduce vibrations from the pumps and to maintain a fixed alignment relative to the optical table containing the laser. The key parameter is the power circulating in the enhancement cavity, which is the product of the cavity enhancement and the input power assuming very efficient mode matching. This product is only 28 mW in our experiments. Our eventual goal was 10 W, which is a factor of 360 more than we obtained, and we do not see a reasonable approach to close this gap. In conclusion, the combination of potentially a factor of 1000 shortfall in the predicted excitation cross-section and this large gap in the technology leads to our recommendation that this approach not be pursued any further.

References

Cannon BD. 1999. *Model Calculations of Continuous-Wave Laser Ionization of Krypton*. PNNL-12253, Pacific Northwest National Laboratory, Richland, Washington.

Cannon BD and GR Janik. 1988. "Resonance ionization of Kr metastables using a single-frequency laser." *Resonance Ionization Spectroscopy 1988.* Inst. Phys. Conf. Ser. No. 94, TB Lucatorto and JE Parks, eds. Institute of Physics, Bristol, England.

Cannon BD, WL Glab, and R Ogorsalek-Loo. 1993. "Photoionization cross section of the $4p^5$ 5d[7/2] J=4 state and radiative lifetimes of three states of Kr I." *Phys. Rev*. A47**:**147-152.

Chang RSF, H Horiguchi, and DW Setser. 1980. "Radiative Lifetimes and Two-Body Collisional Deactivation Rate Constants in Argon for Kr($4p^5$ 5p) and Kr($4p^5$ 5p′) States." *J. Chem. Phys*. 73:778.

Kau R, ID Petrov, VL Sukhorukov, and H Hotop. 1998. "Experimental and theoretical cross sections for photoionization of metastable Ar^* and Kr^* atoms near threshold." *J. Phys. B: At. Mol. Opt. Phys*. 31:1011-1027.

Siegman AE. 1986. *Lasers*, Chapter 17. University Science Books, Mill Valley, California.

Small-Warren NE and LYC Chiu. 1975. "Lifetime of the metastable $^3P_2$ and $^3P_0$ states of the rare-gas atoms." *Phys. Rev*. A11:1777-1783.

Trickl T, MJJ Vrakking, E Cromwell, YT Lee, and AH Kung. 1989. "Ultrahigh-resolution (1+1) photoionization spectroscopy of Kr I: Hyperfine structures, isotope shifts, and lifetimes for the n=5,6,7 $4p^5$ ns Rydberg levels." *Phys. Rev. A,* 39**:**2948-2955.

Wacker JF and BD Cannon. 1991. *Krypton Metastable Production*. PNL-7886, Pacific Northwest Laboratory, Richland, Washington.

Whitehead CA. 1992. Ph.D Thesis, University of Texas at Austin.

Distribution

No. of Copies

OFFSITE

Robert F. Shannon
232 Westbourne Loop
Burbank, WA 99323

3 S. A. Schubert
U.S. Department of Energy
Office of Nonproliferation &
National Security (NN-20)
1000 Independence Avenue SW
Washington, DC 20585

No. of Copies

ONSITE

DOE Richland Operations Office/STP

R. L. Stutheit	K8-50

18 Pacific Northwest National Laboratory

N. E. Ballou	P7-07
B. D. Cannon (10)	K5-25
R. G. Clemmer	K6-48
J. F. Wacker	P7-07
Information Release Office (5)	K1-06